European Journal of Neuroscience, Vol. 14, pp. 1881–1896, 2001

Neural interactions between motor cortical hemispheres during bimanual and unimanual arm movements

S. Cardoso de Oliveira,* A. Gribova, O. Donchin,† H. Bergman and E. Vaadia
Department of Physiology and the Interdisciplinary Center for Neural Computation, The Hebrew University, Hadassah Medical School, P.O.B. 12272, Jerusalem 91120, Israel

Keywords: bimanual coordination, corpus callosum, interhemispheric interactions, local field potentials, motor cortex

Abstract

Cortico-cortical connections through the corpus callosum are a major candidate for mediating bimanual coordination. However, aside from the deficits observed after lesioning this connection, little positive evidence indicates its function in bimanual tasks. In order to address this issue, we simultaneously recorded neuronal activity at multiple sites within the arm area of motor cortex in both hemispheres of awake primates performing different bimanual and unimanual movements. By employing an adapted form of the joint peri-stimulus time histogram technique, we discovered rapid movement-related correlation changes between the local field potentials (LFPs) of the two hemispheres that escaped detection by time-averaged cross-correlation methods. The frequency and amplitude of dynamic modifications in correlations between the hemispheres were similar to those within the same hemisphere. As in previous EEG studies, we found that, on average, correlation decreased during movements. However, a subset of recording site pairs did show transiently increased correlations around movement onset (57% of all pairs and conditions in monkey G, 39% in monkey P). In interhemispheric pairs, these increases were consistently related to the mode of coupling between the two arms. Both the correlations between the movements themselves and the interhemispheric LFP correlation increases were strongest during bimanual symmetric movements, and weaker during bimanual asymmetric and unimanual movements. Increased correlations occurred mainly around movement onset, whilst decreases in correlation dominated during movement execution. The task-specific way in which interhemispheric correlations are modulated is compatible with the notion that interactions between the hemispheres contribute to behavioural coupling between the arms.

Introduction

Movements involving different joints or limbs can require precise coordination of the timing and magnitude of activation of multiple sets of muscles. How this is achieved by the nervous system remains an unresolved question. One particular example of motor coordination, movements requiring simultaneous use of both arms or hands (bimanual movements), has been intensively investigated. Movements of the two arms have the tendency to produce spatially (symmetric) and temporally (phase-locked) similar movements (Kelso *et al*., 1979; Kelso, 1984; Franz, 1997). On the other hand, humans can be trained to produce complex combinations of bimanual movements without these symmetries, such as piano playing. What is the neurophysiological substrate of the linkage connecting the arms, and how is it overridden in bimanual tasks that require their independence? A number of studies suggest that the neocortex and, in particular, callosal interconnections between the hemispheres, may be involved in coordination of the upper limbs. Interhemispheric interactions are enhanced during bimanual learning (Andres *et al*., 1999), and split-brain patients (lacking direct interhemipheric connections) have difficulties learning novel patterns of spatial bimanual coordination (Preilowski, 1972, 1975; Franz *et al*., 2000). They also have considerably fewer problems than normal individuals in producing simultaneous but very different movements of their two hands (Eliassen *et al*., 1999; Franz *et al*., 1996). Although some studies found intact temporal coupling in split-brain patients (Tuller & Kelso, 1989; Franz *et al*., 1996; for review see Donchin *et al*., 1999), a newer report also showed deficits in the temporal domain (Eliassen *et al*., 2000).

Aside from these observations, little is known about the physiological mechanisms underlying bimanual coordination and interhemispheric interactions. Early work using a finger-tapping task (involving only distal muscles) supported the classical view that activity in primary motor cortex (MI) reflects mainly contralateral movements and is hardly affected by whether the movement is unimanual or bimanual (Tanji *et al*., 1987, 1988). More recently, however, two groups investigated the physiology of bimanual movements of the whole arm (involving proximal muscles), and both found, in different paradigms, that neuronal activity in MI could not be accounted for by the activity evoked during their unimanual components (Donchin *et al*., 1998; Kermadi *et al*., 1998). Whilst these results support the hypothesis that MI is involved in coding bimanual arm movements, they do not provide insight into the interactions between concurrently planned movements of the two arms. The present study addresses these interactions. We simultaneously recorded electrical activity from multiple sites within the motor cortex of both hemispheres. Local field potentials (LFPs) and

Correspondence: Dr Simone Cardoso de Oliveira, at *present address below. E-mail: cardoso@arb-phys.uni-dortmund.de

**Present address*: Institut für Arbeitsphysiologie an der Universität Dortmund, Ardeystr. 67, D44139 Dortmund, Germany

†*Present address*: Department of Biomedical Engineering, Johns Hopkins University, 720 Rutland Ave. 416 Taylor Bldg., Baltimore, MD 21205, USA

Received 4 June 2001, revised 28 September 2001, accepted 8 October 2001

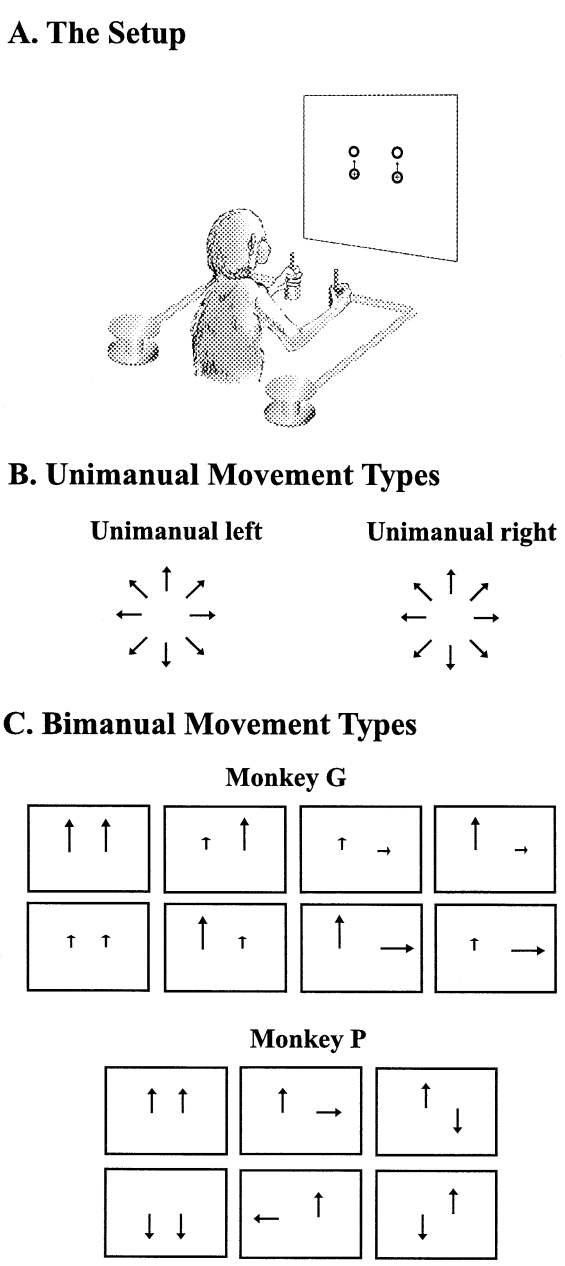

FIG. 1. The behavioural task. (A) The monkey moved two manipulanda in the horizontal plane. The position of each manipulandum was displayed as a cross-shaped cursor on a vertical screen in front of the monkey. Each trial began by presenting two origin circles in the middle of the display (circles with crosses). After the monkey placed the cursors into the origins and held them immobile for a constant delay, the origin circles went off and two target circles appeared at different locations. As an example, the display for a bimanual parallel movement of the same direction and amplitude is sketched. In unimanual trials, one circle appeared in the same location as the origin (for the nonmoved hand). The other circle was displaced from the origin in one of the eight directions shown in B. (C) Schematic representation of the bimanual movements used in our task. For monkey G, movements consisted of moving both arms to the front, or movements in which the two arms were moved in perpendicular directions. In addition, movements of different amplitudes were tested, and all possible combinations of short and long movements were used. In monkey P, we used only movements of the same amplitude. Directions were either the same, perpendicular or opposite. Upward arrows in B and C correspond to forward movements of the monkey, and downward arrows to backward movements towards the chest of the monkey.

single-unit activity were recorded from each electrode (Mitzdorf, 1994). This paper focuses on the LFP signal, which represents the grand average of the synaptic input to the local cortical network in the vicinity of the recording electrode. The data analysis is aimed at evaluation of interactions between neuronal populations as reflected in the LFP signal and their relationship to coordination of bimanual movements. Part of this study has been published in abstract form (Cardoso de Oliveira *et al*., 2000).

Methods

Behavioural paradigm

Two female rhesus monkeys (*Macaca mulatta*; monkey G, 3.5 kg, and monkey P, 4 kg) were trained to move two separate manipulanda, one with each arm. The experimental setup and the principle of the task design are described in Donchin *et al*. (1998). A sketch of the monkey engaged in performance of the task is shown in Fig. 1A. Each manipulandum was a low-weight, low-friction, two-joint mechanical arm, moveable only in the horizontal plane. Movement of each manipulandum caused movement of a corresponding cursor on a vertically orientated 21-inch video screen located ≈ 50 cm in front of the monkey. The movement of each cursor was mapped to its corresponding manipulandum movement such that each millimeter of manipulandum movement caused one millimeter of movement of the cursor on the video display.

The time course of typical unimanual and bimanual trials was as follows. A trial began when the monkey placed both cursors within 0.8 cm diameter 'origins' (Fig. 1A) and held them still for 500 (monkey G) or 1000 ms (monkey P). For each arm, a target (also 0.8 cm diameter) could appear at a distance of 3 cm (monkey P) from the origin. For monkey G, targets could occur at long (5 cm) or short (2.5 cm) distances from the origins. If only one target appeared, signalling a unimanual trial, the monkey moved the appropriate arm and brought the corresponding cursor into the target, but did not move the other arm. If two targets appeared, signalling a bimanual trial, the monkey moved both arms such that the two cursors moved into the targets on the screen. Three types of bimanual movements were studied: parallel, opposite and perpendicular. The types of bimanual trials used during recordings are shown in Fig. 1C. Note that for monkey G the bimanual movements could also entail movements of different amplitudes, but opposite movements were not included. Unimanual movements comprised movements in eight different directions (in all four cardinal directions, plus those directions 45° from the cardinal directions; Fig. 1B). For monkey G we also included long unimanual movements which were components of the bimanual movement types.

The monkey's reaction time was not restricted, but targets had to be reached within 1 s (monkey G) or 1.5 s (monkey P) from target appearance. For bimanual trials, the animal was additionally required to begin movement of the arms within a maximal interarm interval (IAI) of 200 ms and the targets had to be reached with an IAI of 400 ms. Following acquisition of the targets, the monkey held both arms still in the target circle for at least 500 ms. No intertrial interval was imposed. Every second or third successful trial was rewarded with a liquid reward and followed by a 2-s pause to allow for its consumption. In all sessions, trials were presented pseudo-randomly without any separation into blocks. In monkey P, we introduced an additional criterion for successful trials in order to limit spatial intertrial variability in movement execution. This criterion checked whether movement paths were within a narrow straight virtual 'tunnel' connecting the origin and the target circle. The width of this

path was the same as the target circle diameter. This criterion eliminated deviations in movement direction, particularly those leading to curved movements. Because successful performance was more difficult under these conditions, monkey P had lower success rates than monkey G (see Results).

In addition to this behavioural paradigm, we tested the monkeys' hand preferences in a 'raisin board' task. The monkey sat in the primate chair and faced a rectangular Perspex board containing 10 wells of ≈ 3 cm in diameter, arranged in two rows of five wells with a raisin in each well. The board was positioned in the middle, ≈ 30 cm in front of the monkey's chest. The monkey rapidly collected all raisins from the wells. The behaviour of the monkey in this task was taped on video, and we counted how often the monkey used each hand to retrieve the raisins.

Surgery

After training, we implanted a recording chamber (27 × 27 mm) above each hemisphere, and a head holder was attached to the occipital bone. The surgery was performed under general anaesthesia and aseptic conditions. Magnetic resonance images (taken in a Biospec Bruker 4.7-Tesla animal system, fast-spin echo sequence; effective TE = 80 ms and TR = 2.5 s, 13 coronal slices 2 mm wide) aided in placement of the chambers. In Monkey P, the position of the recording chambers and the orientation of two electrodes that were inserted through the chambers into the brain were verified by a second MRI session after surgery. The animals' care and all surgical procedures were in accordance with the NIH *Guide for the Care and Use of Laboratory Animals* (rev. 1996) and all applicable Hebrew University regulations.

Recording

During recording sessions, the monkey was seated in a primate chair placed in a dark chamber with its head fixed. Single-unit activity and LFPs were recorded by eight glass-coated tungsten microelectrodes (impedance 0.2–0.8 MΩ at 1 kHz) in the two hemispheres (four electrodes in each hemisphere). Electrodes were driven into each hemisphere through eight tubes that were tightly fitted into a metal guide, with seven of the tubes forming a circle and one in the middle. The horizontal distance between the four electrodes we inserted could be either ≈ 350, ≈ 600 or maximally ≈ 700 μm, depending on the relative positions in the guide. In normal placements, only two electrodes were spaced at the minimal distance, and the others were spaced at the intermediate or maximal distance. Electrodes were individually driven to allow optimal isolation of spiking activity. Therefore, the difference in depth between electrodes could vary from one session to another. The electrode signals were amplified and filtered by a multichannel analogue data processor (MCP, Alpha-Omega, Nazareth, Israel). The raw wideband signal was subjected to two different ranges of band-pass filters in order to yield spike activity (filtered between 300 Hz and 8 kHz) and LFP signals (filtered between 1 and 150 Hz). The LFP data were sampled at 400 Hz and stored on disk. As reference we used a grounded metal screw, which was implanted into the skull and connected by conductive wires that were wrapped around all screws that held the two chambers. Pick-up of mechanical or electrical noise was minimized by mechanically attaching the drives and head stages to the implanted chambers.

Fifty Hertz noise caused by the a.c. power line was attenuated using a digital notch filter applied off-line (49.8–50.2, 99.8–100.2 and 149.8–150.2 Hz four-pole Butterworth filter, applied forward and backward to prevent phase shifts).

Selection of recording sites

At each penetration coordinate, four electrodes were advanced into the brain. After penetrating the dura, electrodes were separately advanced until well-isolated units were detected. Recording sites were not especially selected for activity related to movements, but for the occurrence of stable single-unit recordings (as judged by stability of spike amplitude and spike rate). LFP channels numbered 0–3 were always recorded by microelectrodes in the right hemisphere, and channels numbered 4–7 were recorded in the left hemisphere. At the end of each recording session, we tested for neuronal responses to passive manipulation and tactile stimulation of the limbs, tail, trunk and head. Evoked activity was evaluated by listening to the amplified spike signal passed directly into a loudspeaker. Finally, we applied intracortical microstimulation (ICMS) with 50-ms trains of 200-μs cathodal pulses at 300 Hz with an intensity of 10–80 μA (BPG-2 and BSI-2, BAK Electronics, Germantown, MD, USA). When ICMS evoked movements, we documented the movements evoked and the threshold stimulation intensity. Stimulation and passive manipulation were performed at the end of each recording session, as well as in dedicated mapping penetrations. For this study, we only included recording sites that were well within the arm representation, as determined by passive stimulation and microstimulation.

After completion of recordings, monkey G was killed with an overdose of Nembutal ® and perfused transcardially by 0.9% saline and paraformaldehyde fixative solution (4% paraformaldehyde in 0.1 M phosphate buffer). The brain was removed and photographed, sunk in sucrose, sliced on a cryostat (50 μm section width) and Nissl-stained with Cresyl Violet. Penetration positions were confirmed to be in the motor cortex by mapping them onto the surface of the brain using the chamber coordinates and positions. All our recordings were from the exposed surface of the precentral gyrus. Most of the sites were in primary motor cortex, but some of the more anterior sites were located at the border to the caudal portion of dorsal premotor cortex. Monkey P is still participating in experiments. Therefore, the locations of the recording sites in monkey P were determined by magnetic resonance images. During imaging, we placed microelectrodes into the brain at known chamber coordinates. In this way, the anatomical positions of the microelectrodes could be confirmed as lying within the motor cortex.

Data analysis

All recording sites were assessed for intertrial stability of LFP signals and for the occurrence of excessive noise. Recordings with recurring artifacts, and those with strong 50 Hz noise persisting after off-line filtering, were excluded from analysis. We also excluded portions of the data in which the LFP recordings changed considerably across trials (e.g. baseline shifts or changes in noise level). No selection was made on the basis of whether or not sites displayed task-related activity.

All LFP traces were aligned upon the beginning of movement, determined by an off-line algorithm, and double-checked manually. The movement initiation detection algorithm (courtesy of A. Arieli) calculated the zero intercept of a line passing through two points on the velocity profile. One point was at 2/3 of the peak speed and the other was at 1/3 of peak speed. It also included corrections for different special cases of unusual velocity profiles. In order to determine movement duration, the end of movement was detected similarly. For purposes of alignment, the beginning of movement in bimanual trials was determined by the first arm to begin moving. We

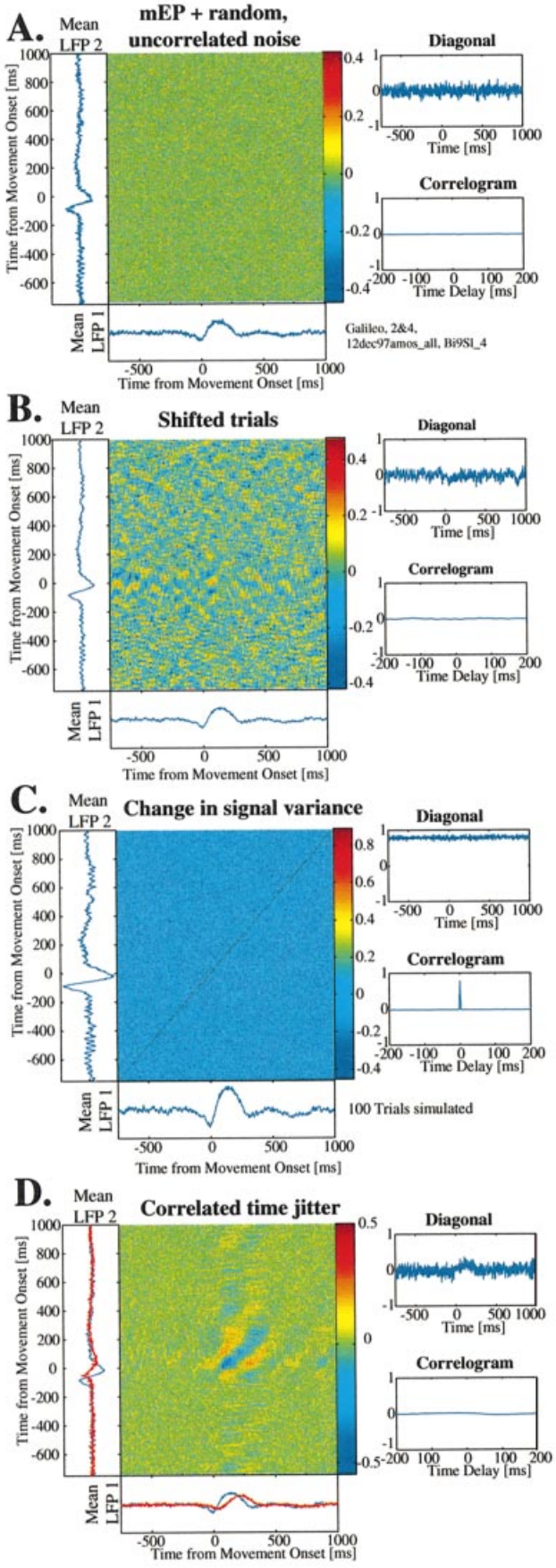

call the average of all aligned LFP signals recorded during identical movement types the mean motor evoked potential (mEP; see Fig. 3B).

Determining preferred directions (PDs) of LFPs

In order to determine the preferred direction of the LFPs recorded from a given site, we measured the peak-to-peak size of the mEP by calculating the distance between the maximum and the minimum of the mEP. Out of the eight directions movements of the contralateral arm, we constructed a tuning curve of these peak-to-peak values (observed tuning). We fit a cosine to these eight points using a simple least-squares fit to the equation:

$$PTP(\theta) = A \cdot \cos(\theta - PD) + B, \theta = 0°, 45°, \ldots, 315° \quad (1)$$

θ is defined such that 0° corresponds to movements to the right, and angles proceed in a counterclockwise direction. We extracted the direction of the maximum of the cosine function (PD) and the goodness of fit, as measured by r^2 (the variance of the fit divided by the variance of the original model). If the r^2 value exceeded 0.6, we considered the LFP to be significantly tuned.

Cross-correlation analysis

As a first approach towards studying correlations between LFPs, we calculated time-averaged cross-correlograms between LFP channels. We applied this analysis to two different epochs of the trial. The first was the interval between 750 and 250 ms before movement onset, during which the monkey held its hands stationary at the origins and waited for the target (or targets) to appear. We call this time window the hold period. The second window contained the time from 250 ms

FIG. 2. Various controls of the joint peri-event time correlogram (JPETC) technique. (A) The mEP does not result in spurious correlations within the JPETC. To create the JPETC displayed here, two sets of sham data were created with independent, random, normally distributed noise around the mEPs. The means (over all trials, = mEPs) of the two signals are shown along the lower and left border of the JPETC. Each pixel in the JPETC represents the correlation coefficient between all the (single-trial) values of the first local field potential signal (LFP1) at the corresponding time bin of the *x*-axis and the values of LFP2 at the respective time bin of the *y*-axis. Correlation is expressed as correlation coefficient and is shown in a colour code, with the colour scale given on the right side of the JPETC. The plot labelled 'diagonal' shows the values of the JPETC main diagonal. By averaging the values of the JPETC diagonals corresponding to the delay range of –200 to +200 ms, one obtains one value for each time delay, and these values are shown in the plot labelled 'correlogram'. (B) Correlating time-shifted trials with each other does not result in correlations in the JPETC. The shifting procedure was done by correlating subsequent trials with each other, and the last trial with the first one. The JPETC of the shifted data does not show any clear structure. Both the main diagonal and the correlogram show only random fluctuations. In contrast, the nonshifted data (see Fig. 7B) show a clear, transient correlation along the main diagonal. (C) Modifying signal variance without changing the correlation coefficient does not disrupt the correct calculation of correlation strength. Sham data with fixed correlation coefficient (0.8, obtained by adding a mixture of independent and dependent noise to the mEP) and a step in signal variance (from 0.3125 to 1.125, at the time –250 ms) have been created and subjected to the JPETC method. The correlation coefficient at zero delay correctly indicates a value of 0.8 which is constant over time. (D) Correlated time jitter in the LFP signals induces patterns in the JPETC. Sham data have been created in which the mEP was shifted in time by a random delay (mean, 0 and SD, 100 ms), which was identical for both signals. After time shifting, random uncorrelated noise was added to the signals. The correlated time jitter results in a structure in the JPETC and the main diagonal shows a small transient increase at the time of the mEP. The mEP of the original data is shown in blue, whilst the mEP of the surrogate data is shown in red. Because of the time jitter, the mEP is smeared out in the surrogate data.

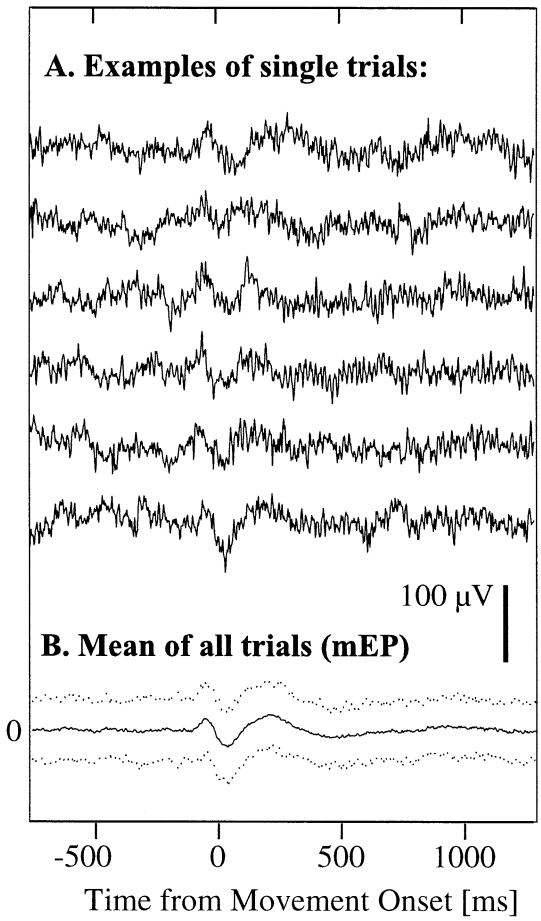

FIG. 3. Examples for LFP recordings during (A) single trials and (B) the mean over all 79 trials recorded for this movement type, yielding the motor evoked potential (mEP). The dotted lines in B represent the mean ± 3 SD. The traces in A and B are plotted in the same voltage resolution in order to highlight size relationships between the signals.

before to 1000 ms after movement onset, during which motor preparation and movement execution occurred. We call this time window the movement period. For all possible pair-wise combinations of simultaneously recorded LFPs, we calculated the correlograms obtained during these two time windows, using time delays between –200 and +200 ms, and a bin width of 2.5 ms, which was our sampling resolution. To this end, we used the Matlab xcorr function (MatLab, MathWorks, Natick, MA, USA), with correlation expressed as the correlation coefficient. The correlogram of a single trial is defined by the following equation:

$$CC(\tau) = \frac{\sum_{t=1}^{T} \left[LFP1(t) - \overline{LFP1}\right] \cdot \left[LFP2(t+\tau) - \overline{LFP2}\right]}{\sqrt{\sum_{t=1}^{T} \left[LFP1(t) - \overline{LFP1}\right]^2 \cdot \sum_{t=1}^{T} \left[LFP2(t+\tau) - \overline{LFP2}\right]^2}}, \quad (2)$$

where τ is the time delay between the signals, t is the time bin out of T total time bins and a bar above *LFP1* or *LFP2* indicates the average of each trial.

The correlograms obtained for all trials recorded under the same conditions (during the same movement type or during the hold period) were averaged to reduce noise. Examples for such correlograms, obtained from the hold period, are shown in Fig. 5. From each correlogram, we determined the maximum value. Negative correlations constituted only ≈ 1% of our total sample and were not analysed separately. For correlation peaks > 0.1, we also determined the time lag of maximum correlation.

The conventional cross-correlation is affected both by similarities of the average signals (which, during the movement period, correspond to the mEPs) in the two electrodes and by possible trial-wise interactions between the single trial signals. A common way to distinguish between these two aspects is to calculate a 'shift predictor' to approximate the correlation between the averages, and then subtract it from the correlograms to derive an estimate of the 'pure' trial-wise correlation. We calculated the shift-predictor by correlating the i-th trial of one electrode with the $(i + 1)$-th trial of the other, and the last trial with the first trial.

The shift predictor was also used to define a confidence limit for oscillatory components in cross-correlograms. As a confidence limit for oscillatory correlation, we chose the mean (over all delays) of the predictor ± 3 SD (again, over all delays). Whenever we found at least one satellite peak (on each side of the main correlogram peak) which exceeded these values, we scored a correlogram as having a significant oscillatory component.

The joint peri-event time correlogram (JPETC)

To study the temporal aspects of the modification of correlation strength, we used a dynamic correlation method, based on the joint peri-stimulus time histogram (JPSTH), developed by Aertsen and coworkers for single-neuron data (Aertsen *et al.*, 1989). We adapted this method to LFP signals and produced the JPETC. The JPETC is a matrix of the correlation coefficients of two analogue channels for all possible combinations of paired time lags relative to an external event. We calculated the JPETC in an epoch starting 750 ms before movement onset and continuing to 1000 ms after movement onset. Using a time resolution of 2.5 ms, there were 700 bins in each segment. The correlation coefficients were calculated using the equation:

$$CC(t_1, t_2) = \frac{\sum_{n=1}^{N} \left[LFP1_n(t_1) - \overline{LFP1(t_1)}\right] \cdot \left[LFP2_n(t_2) - \overline{LFP2(t_2)}\right]}{\sqrt{\sum_{n=1}^{N} \left[LFP1_n(t_1) - \overline{LFP1(t_1)}\right]^2 \cdot \sum_{n=1}^{N} \left[LFP2_n(t_2) - \overline{LFP2(t_2)}\right]^2}}, \quad (3)$$

where t_1 is the time bin from LFP1, t_2 is the time bin from LFP2, and n is the n-th trial out of a total of N. A bar over *LFP1* or *LFP2* in Eqn 3 indicates that the mean should be taken across trials (thus, $\overline{LFP1}$ and $\overline{LFP2}$ are mEP1 and mEP2). The result takes the form of a 700 × 700-bin matrix constituting all possible time delays between LFP1 and LFP2. For example, the values corresponding to the simultaneous (zero-delay) correlation are situated along the main diagonal of this matrix. Figures 2 and 6–8 give examples of JPETC matrices displayed using a colour-coded flat display. Time progresses from the bottom left to the top right corner such that the value of t_1 (the time index of the first LFP) increases along the x-axis and the value of t_2 (the time index of the other LFP) increases along the y-axis. Finally, averaging all diagonals from bottom left to top right yields a cross-correlogram. Because of differences in normalization, however, this correlogram is not identical to the one obtained by the classical cross-correlogram technique mentioned above. The bin-wise

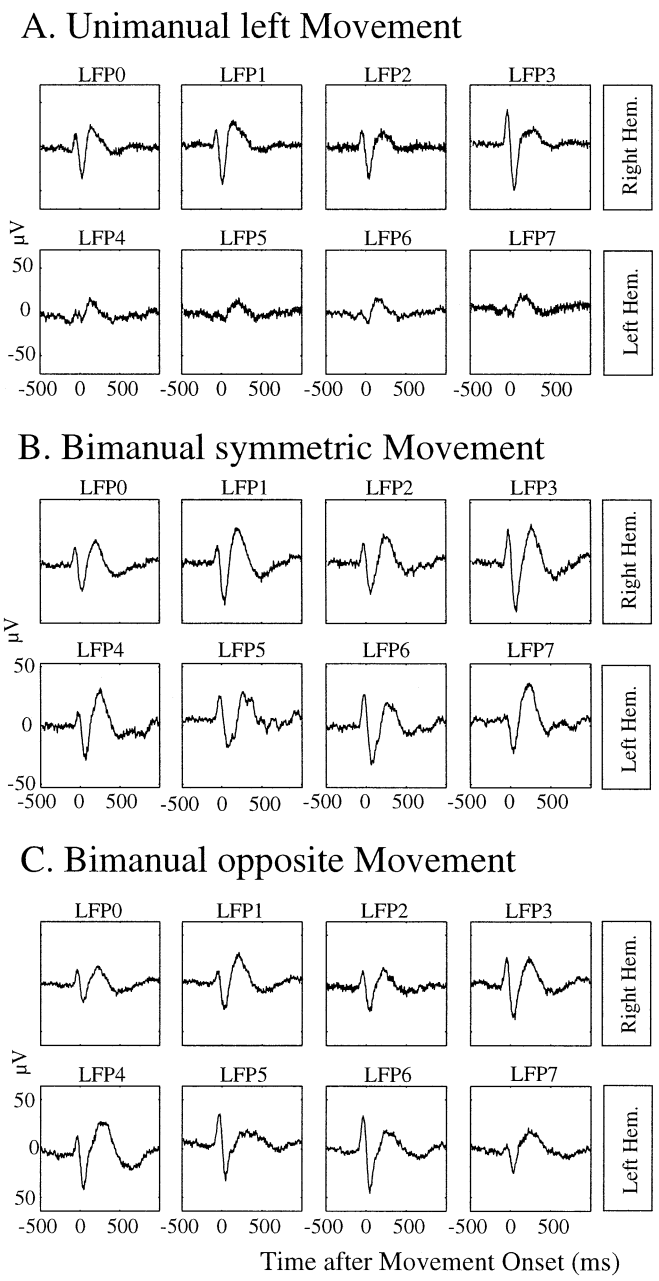

FIG. 4. Examples for mEPs recorded simultaneously in one recording session during different movement types. Local field potentials (LFPs) 0–3 were recorded in the right hemisphere, LFPs 4–7 in the left hemisphere. In unimanual movements, mainly the electrodes in the contralateral hemisphere are activated, although smaller activation can also be observed in the ipsilateral hemisphere. During bimanual movements, both hemispheres are active. Notice that the shape of mEPs is similar between electrodes and remains relatively constant, whilst its size is more strongly affected by the movement type to be executed.

significance of the correlation coefficients in the JPETC was determined by testing against the hypothesis that the correlation coefficient is 0, using a standard *t*-test.

Theoretically, the JPETC procedure should result in correlation values that are not contaminated by similarities in the evoked potentials of the two signals. We checked that this was the case using two different tests. First, we applied the JPETC algorithm on sham data with similar time-dependent mean waveforms and uncorrelated additive trial-by-trial noise. We created 103 trials of two such sets of sham data by randomly drawing, for each trial and each time bin, a value from a normal distribution with the same mean and SD, as observed in two sets of real data. As expected, this procedure resulted in JPETC-displays without any structure (Fig. 2A). Both the diagonal and the correlogram (calculated by averaging the diagonals) were flat. Whilst these random sham data replicated the similarities of the means over all trials (the mEPs), they did not have the same temporal structure within a trial as the real data.

As a second method, we calculated a shift-predictor for the JPETC by correlating signals between subsequent instead of simultaneous trials (and the last trial with the first trial). Figure 2B shows the result of this procedure. For comparison, the JPETC of simultaneous trials data are displayed in Fig. 7B. Although the evoked potentials are identical, as they must be, the shifted JPETC displays no correlation whatsoever, either in the JPETC itself or in the average cross-correlogram. In contrast, the original data do show a clear correlation along the main diagonal, which is strongly modulated around the time of movement onset.

Third, we addressed the possible concern that the JPETC may be sensitive to changes in signal variance. It has been observed that, during evoked potentials, the variance of cortical activity is usually reduced slightly by about 10–20% (A. Arieli, unpublished observations). In order to check whether a change in variability could lead to a change in correlation strength observed in the JPETC, we created sham data in which the correlation coefficient between the two signals was held constant but the variance of the individual signals was increased or decreased over time. We found that the JEPTC faithfully reflected the correlation coefficients and was not influenced by a change in variance (Fig. 2C).

When analysing spike data with the JPSTH technique, it has been shown that intertrial covariations in neuronal excitability and response latency can produce patterns of correlations in the JPSTH (Brody, 1999; Baker & Gerstein 2001; Ben-Shaul *et al.*, 2001). This intertrial covariability will not show up in the shift predictor. As a result, when interpreting the JPSTH one has to take into account that its features could be caused by either 'real' spike timing correlations or by intertrial covariability. We have tested the effect of intertrial covariations on the JPETC method of analogue data. To simulate covariations in signal amplitude, we created surrogate data by adding random, independent noise to two mEPs which were randomly scaled in each trial by a common factor. The JPETC of these data showed no features along the diagonal (not shown). The fact that we observed practically no effect of size covariability in our data may be related to the range of size scaling that we applied (we used an SD of 0.3, creating mEPs which varied in size between 0 and 2 times the original amplitude). This range is reasonable for LFP data, because the amplitude range of variabilities in the LFP does not exceed twice the amplitude of the mean signal. It is possible that the more profound impact on the JPSTH of spike data emerges due to the higher intertrial variability of the spike responses. We thus conclude that covariations in signal velocitiy do not seem to play a major role in the JPETC of LFPs.

Next, we assessed the possibility that covariability in signal timing could affect the JPETC. In sensory systems, variability in signal timing is caused by variations in response latency. In the motor system, variability in timing is related to a variable time delay between neural activity and the initiation of a movement. We created another set of surrogate data by, again, adding noise to the mEP. This time, for every trial, the mEPs of the two signals were shifted along the time axis in a correlated way (by the same amount of time). The time delay for each trial was randomly chosen from a normal

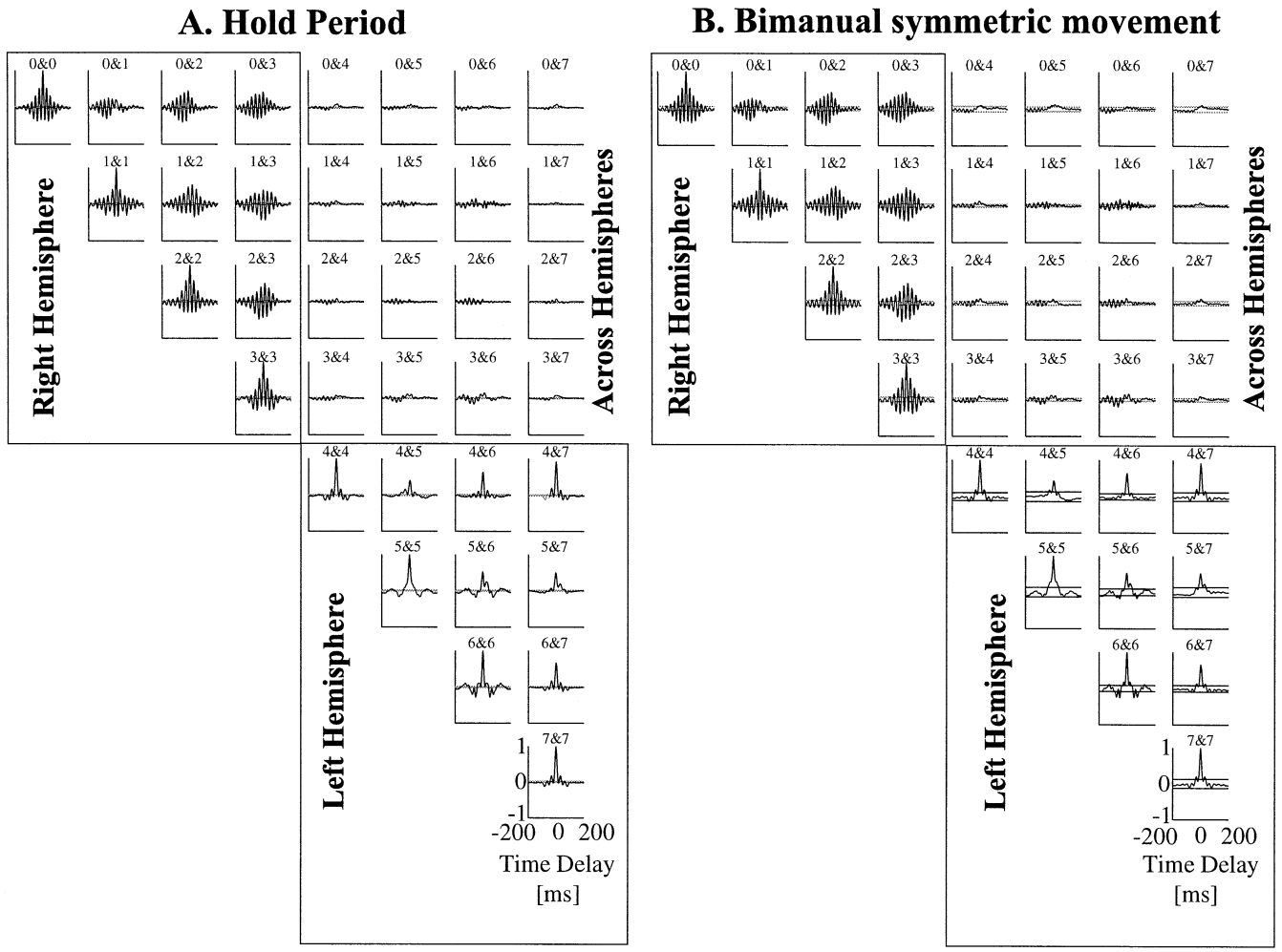

FIG. 5. Mean trial-by-trial cross-correlations among all simultaneously recorded LFPs from one recording session, analysed (A) during the immobile hold period, and (B) during a bimanual symmetric movement to the front. Autocorrelations are included along the diagonal. Note that the correlations between the hemispheres are much smaller than those within the same hemisphere. The differences between corresponding correlograms in A and B are minor. In the right hemisphere, strong oscillations in the gamma range are present. In contrast, alpha-range oscillations predominate in the left hemisphere. Gray lines indicate confidence limits indicating the range of ± 3 SD around the mean of the shift predictor.

distribution. We tested random distributions with various widths (standard deviations; SD), ranging from 25 to 100 ms. Figure 2D shows the result of this procedure with a standard deviation of the time jitter of 100 ms. The correlated timing jitter in the evoked response does induce a pattern in the JPETC which is somewhat similar to the pattern observed for the real data (Fig. 7B). Smaller ranges of time jitter resulted in weaker structures in the JPETC. However, it should be noted that even with the perfectly correlated and large jitters, the strength of the maximal correlation change (as shown in Fig. 2D) was substantially weaker than the one observed in the original data (compare Fig. 7B). We conclude that correlated time jitters in the two signals may contribute to structures within the JPETC, but are clearly not the sole source of them.

In summary, the simulations demonstrate that it is unlikely that the JPETC is contaminated by the sizes or shapes of the mEPs or by overall changes in variability. It rather reveals correlations between the trial-by-trial fluctuations of the two LFP signals around the mEPs, but may also reflect covariations in signal timing. Both phenomena are interesting, because they reflect interactions caused by the underlying network architecture. Changes in correlation patterns can be interpreted as evidence for dynamic changes in the functional network structure, resulting in variable interactions between the local cortical activities at two sites. Covariations in signal timing can be seen as evidence for a common timing linking distant neuronal sites.

Because the strongest correlations and correlation changes occurred at zero time delay, we focused on the main diagonals of the JPETC in further analyses. This diagonal had a width of 1 bin, i.e. 2.5 ms, and also a temporal resolution of 2.5 ms. To test for movement-related changes in correlation, we compared the diagonals during the hold period and the movement period. In order to allow for statistical comparison, we transformed the correlation coefficients on each diagonal using Fischer's z-transform.

We then normalized the diagonals during the movement period by subtracting the mean correlation during the hold period (corresponding to the mean of the first 200 bins, i.e. the first 500 ms of the diagonal) and dividing by the SD within this time. We defined the confidence limit for significant changes as 3 and –3, respectively. These values correspond to deviations of >3 SD from the mean correlation in the hold period. Assuming a normal distribution, this corresponds to a rejection at $P \leqslant 0.002$. To assess the times during which significant correlation changes occurred most frequently, we counted, for each time bin, the

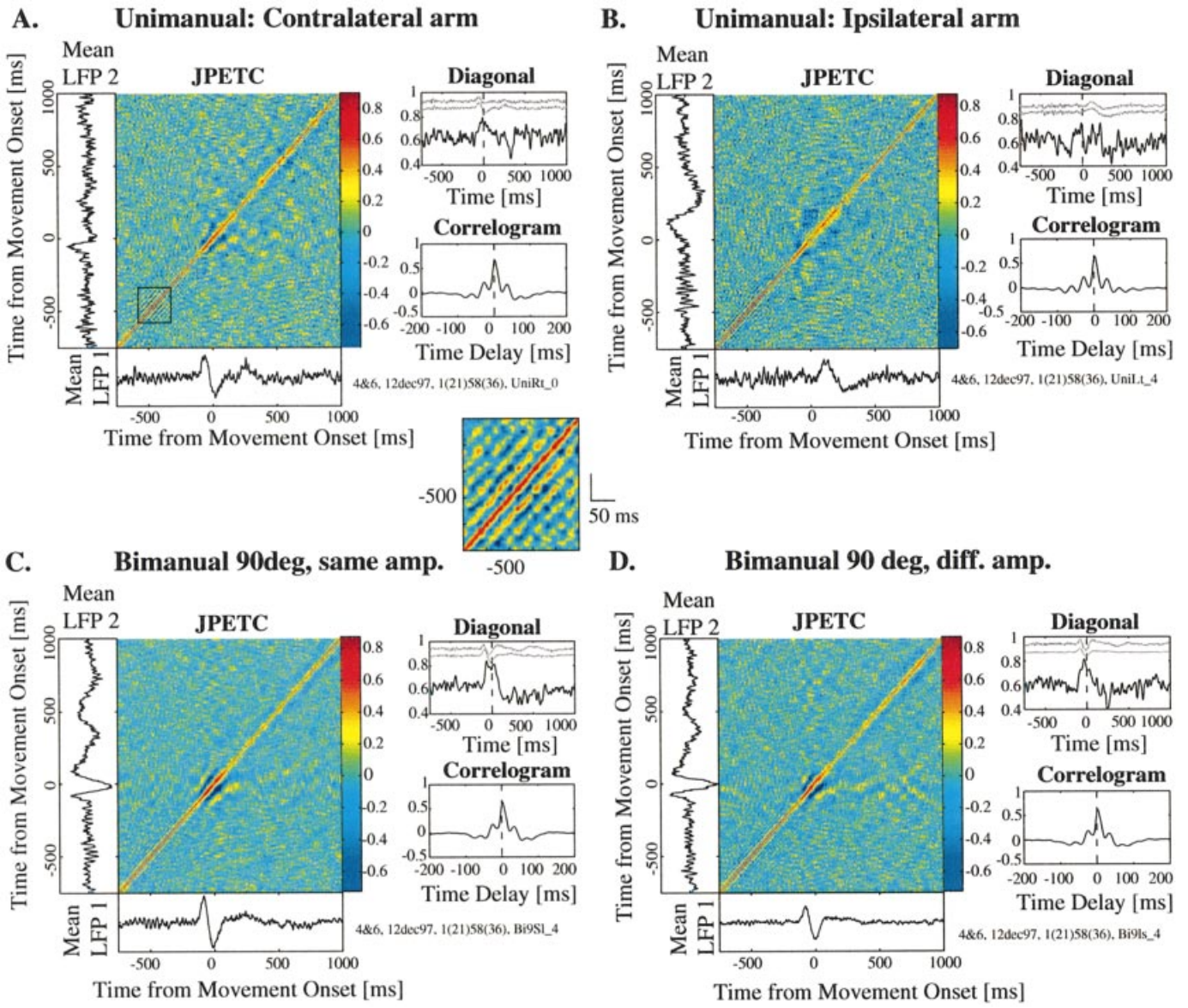

FIG. 6. Time-dependent functional interactions between LFPs during different movement types as revealed by the JPETC technique. This particular example was recorded from the left hemisphere. The plots are arranged in the same way as in Fig. 3. Diagonals have been smoothed by a seven-point averaging filter. In order to compare the time course of correlation changes to the mEPs, the mEPs are inserted in the plot of the diagonal in grey (note that the mEP sizes are scaled differently than the diagonals). Vertical dotted lines mark the time of movement onset and 0 delay correlation. JPETCs (A and B) during unimanual movements and (C and D) during bimanual movements in which both arms are moved simultaneously in the same directions as in A (right arm to the right) and B (left arm to the front). Note that the time scale for the JPETC and the correlogram are different, with the correlogram depicting only 200 bins around the main diagonal.

number of JPETC main diagonals (for all pairs and all conditions) in which values >3 (for increased correlations) or <-3 (for decreases in correlation) occurred.

Results

Behaviour

The monkeys were trained until they performed all movement types reliably and at a stable performance level. In monkey G, $>90\%$ of the unimanual movements were performed correctly and within the timing requirements. Bimanual movements in the same direction were executed with a performance of $>75\%$ correct movements, whilst bimanual movements differing 90° in direction were performed with $>55\%$ correct movements. In monkey P, the average success rate was somewhat lower (60–70% in unimanual trials and 50–60% in bimanual trials), probably because the requirements for successful performance were more strict (see Materials and Methods). Movements were initiated with an average reaction time (from target appearance to movement initiation) of 267 ± 140 ms in monkey G, and 366 ± 42 ms in monkey P. The average movement times (from movement initiation to target acquisition) were 529.6 ± 143.8 ms (monkey P, left arm), 607.0 ± 193.8 ms (monkey P, right arm), and

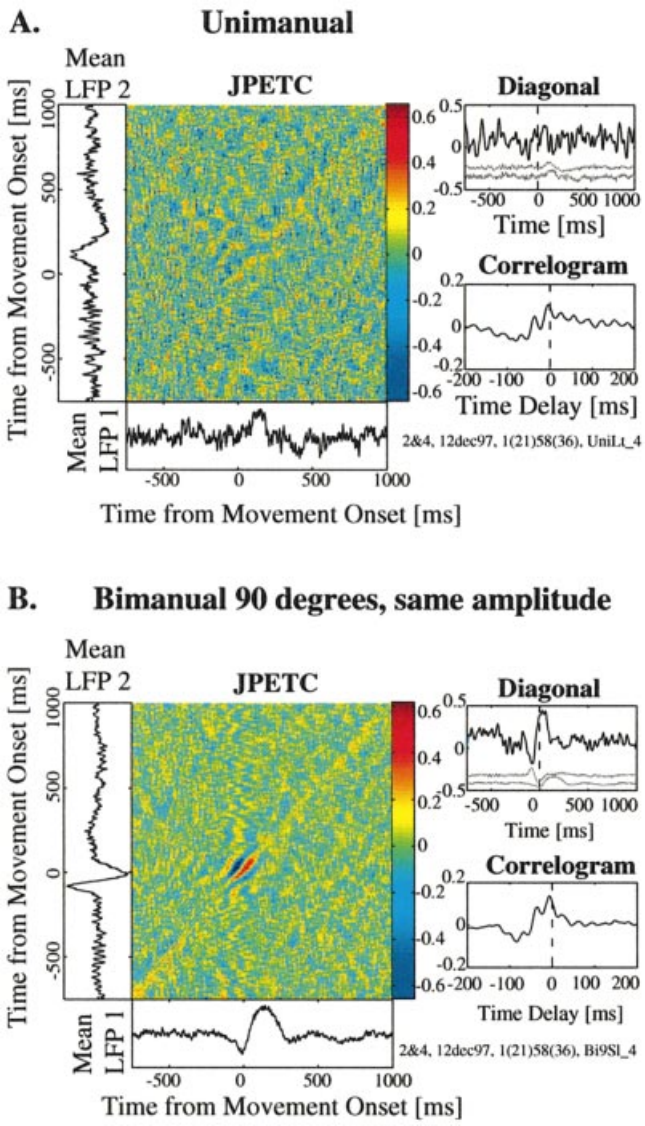

FIG. 7. Example of JPETCs of a pair of recording sites from different hemispheres. (A) The correlation pattern during unimanual movements of the contralateral (left) arm to the front. No correlation is apparent between the two electrodes in this condition. (B) The correlation pattern for the same pair during a bimanual movement of the same amplitude. Movement directions of the two arms differ by 90°, with the left arm moving to the front (as in the unimanual condition shown in A) and the right arm moving to the right. A strong correlation with side peaks arises around movement onset and lasts for ≈ 100 ms.

529.6 ± 143.8 ms (monkey P, left arm), 569.0 ± 195.0 (monkey P, right arm). In bimanual movements, both monkeys started movements of their individual arms almost simultaneously. Although we allowed for a maximal IAI of 200 ms, the actually observed IAIs were considerably smaller (48.8 ± 53.8 ms in monkey G and 1.5 ± 37.6 ms in monkey P). In monkey G, the right hand began the movements before the left in 92% of the movements whilst in monkey P the right hand led in only 56% of the cases. Both monkeys preferred to use the right hand when picking up raisins from the wells in a Perspex board. Monkey G picked up 93% of the raisins with the right hand, and monkey P picked up 82% with the right hand (average over the last 3 days of testing).

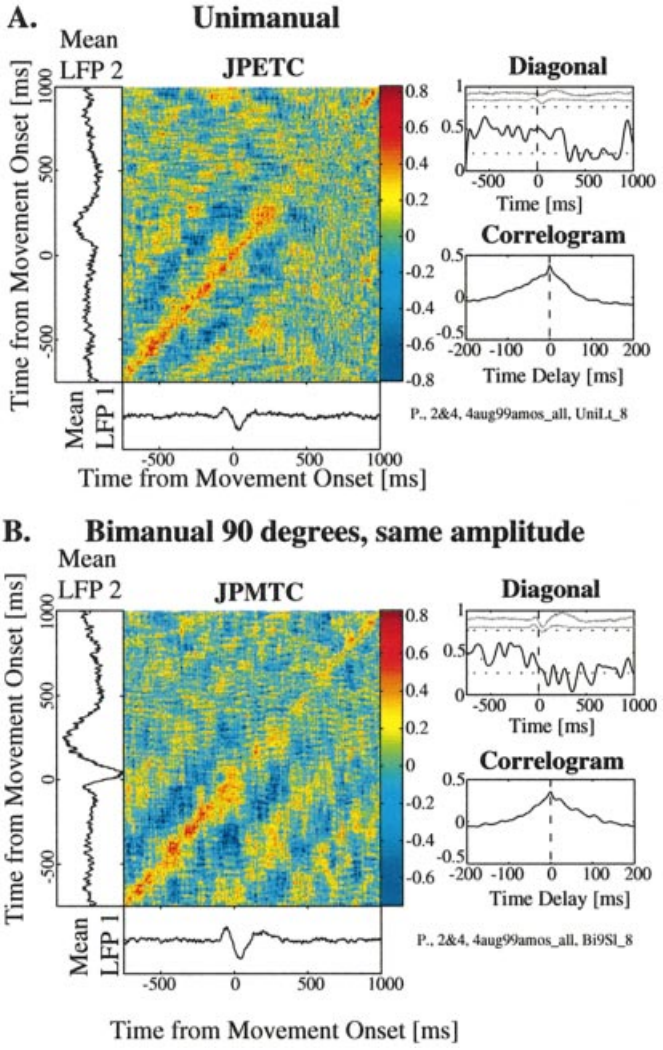

FIG. 8. Example for decorrelations between a pair of recording sites situated in different hemispheres. Data during (A) a unimanual movement of the left arm to the left, (B) during a bimanual movement, with the left arm moving to the left and the right arm to the front. Same format as Figs 2, 6 and 7.

Neuronal activity

LFPs were recorded at a total of 341 recording sites during 88 penetrations in the two monkeys. Out of these, 227 passed our criterion for recording quality (90 in monkey G, 137 in monkey P). All possible combinations of simultaneously recorded sites yielded 648 pairs, 162 within the right hemisphere (69 from monkey G, 93 from monkey P), 120 pairs within the left hemisphere (52 from monkey G, 68 from monkey P), and 366 pairs from different hemispheres (157 from monkey G, 209 from monkey P).

Oscillatory activity

LFP signals frequently contained oscillatory epochs in various frequency bands, in particular in the alpha (8–14 Hz) and gamma (30–55 Hz) range. In some cases, oscillatory activity was strong enough to be observed in the LFP traces of single trials. Significant oscillatory side bands (see Materials and Methods) were present in 34% of the autocorrelograms in monkey G and 33% of the autocorrelograms of monkey P. Crosscorrelograms between the LFPs recorded from different sites also contained oscillatory side bands (see, for example, Fig. 5) in 32% (monkey G) and 16%

TABLE 1. Average peak correlations within, and between, the hemispheres for different movement types

	Average maximal correlation		
	Within right hemisphere	Within left hemisphere	Between hemispheres
Monkey P			
Number of units (*n*)	(130)	(106)	(325)
All trial types	0.57	0.61	0.36
Unimanual right movements	0.54	0.60	0.36
Unimanual left movements	0.58	0.62	0.32
Bimanual movements	0.58	0.59	0.40
Monkey G			
Number of units (*n*)	(78)	(67)	(203)
All trial types	0.37	0.48	0.15
Unimanual right movements	0.37	0.49	0.14
Unimanual left movements	0.39	0.49	0.15
Bimanual movements	0.37	0.47	0.15

Average peak correlations in correlograms from within the right, within the left, or between the two hemispheres during different movement types. Correlation values represent correlation coefficients measured at the maximum of the cross-correlogram.

(monkey P) of the pairs. Pairs within the same hemisphere more often showed significant oscillations than pairs recorded from different hemispheres (45 and 37% as compared to 30 and 11%, in monkeys G and P, respectively).

Mean evoked potentials

Figure 3 shows examples of the LFP in single trials recorded from a site in the arm area of motor cortex during performance of one type of bimanual movement (bimanual parallel movement to the front). Figure 3A shows examples of single trials of LFP recordings, whilst Fig. 3B shows, on the same scale, the average of all 79 trials recorded under this condition, and the average ± 3 SD. The figure demonstrates considerable intertrial variability, which is of the same order of magnitude as the mEP. Similar intertrial variability in population activity has already been reported (Arieli *et al*., 1995; Arieli *et al*., 1996; Tsodyks *et al*., 1999).

Whilst evoked potentials can be identified in most single LFP traces in this particular example, this was not the case for the LFP at all recording sites. In many cases, the evoked potential was only seen after averaging, and there were typically ≈ 100 trials available for each movement type contributing to the average. The shape of the mEP (see also Fig. 4, in which mEPs are displayed in a larger format) shows the same components described previously: a sequence of an initial positive wave followed by large, narrow negative and a broader positive wave and, sometimes, another small negativity (Donchin *et al*., 2001).

Figure 4 illustrates the mEPs evoked in eight simultaneously recorded local field potential signals. LFP 0–3 were recorded from the right hemisphere, LFP 4–7 from the left hemisphere. Typically, the mEPs recorded within the same hemisphere were similar. In unimanual movements, the mEPs were larger in the hemisphere contralateral to the moving hand, although a smaller ipsilateral activation was consistently present (see Fig. 4A). During bimanual movements, large mEP amplitudes were recorded in both hemispheres (Fig. 4B and C). In many cases, the mEP amplitude in bimanual movements exceeded the one during contralateral movements, an effect which we termed bimanual related activity and which is described in detail elsewhere (Donchin *et al*., 2001).

Crosscorrelogram analysis

Crosscorrelograms were calculated for all combinations of recording sites, for the hold period and for each of the different movement types separately. Figure 5 depicts the autocorrelograms (on the diagonal) and cross-correlograms for all LFPs and LFP pairs recorded simultaneously in one session (monkey G). In Fig. 5A, correlograms were constructed from the hold period whilst, in Fig. 5B, the same electrode pairs were analysed during the movement time of bimanual movements to the front. Comparing parts A and B of the figure shows that correlations did not change substantially during movements (see also below, Table 1). Note that, in this particular example, there are strong correlated oscillations of different frequency in each of the hemispheres. The oscillation frequency in the right hemisphere was in the gamma range ($\approx$ 40 Hz), whilst in the left hemisphere, both alpha ($\approx$ 10 Hz) and gamma oscillations were visible. Both the intensity and the frequency range of oscillations varied from one recording site to another. There was no general preference for a certain frequency band in either hemisphere.

Figure 5 demonstrates the general finding that cross-hemispheric pairs were weakly correlated whilst intrahemispheric pairs were strongly correlated. Table 1 demonstrates this for all pairs in our sample. It presents the averaged peak sizes for all pairs, during performance of unimanual and bimanual movements. In both monkeys, the correlations between hemispheres were significantly lower than within the same hemisphere (Wilcoxon rank sum test, $P < 0.001$). Surprisingly, we found a difference in the intrahemispheric correlation strength of the two hemispheres. In both monkeys, correlations within the right hemisphere were significantly smaller than in the left hemisphere (Wilcoxon rank sum test, $P < 0.001$). The time delays associated with maximal correlation strength were centred around zero delay, with a mean of 0 ms (monkey G) and 2.5 ms (monkey P) for intrahemispheric correlations, and –5 ms (indicating that the left hemisphere was leading, monkey G) and 2.5 ms (indicating that the right hemisphere was slightly leading, monkey P) for interhemispheric correlograms. In pairs situated in different hemispheres, the SD of peak delays was considerably higher than for those within the same hemisphere (31 as compared to 20 ms in monkey P, and 58 as compared to 32 ms in monkey G).

In monkey G, the level of interhemispheric correlations was constant and did not show any significant differences between movement types. In monkey P, all bimanual movements elicited slightly higher correlations between the hemispheres than did unimanual movements. Despite its small size, this difference turned out to be significant (Wilcoxon rank sum test, $P < 0.001$). No significant differences among bimanual movement types were found in either monkey. The analysis summarized in Table 1 was repeated after subtracting the shift predictor from each of the correlograms. The results were very similar, but the small difference in monkey P between bimanual and unimanual movements disappeared.

To summarize, the averaged cross-correlograms revealed stronger correlation within hemispheres than correlation between hemispheres, but failed to clearly distinguish among different types of bimanual movements.

Dynamics of correlations: results of the JPETC-analysis

The cross-correlograms of Fig. 5 depict correlations between LFPs averaged over a long time. However, rapid modifications of correlation can easily be eliminated due to this averaging. We used the JPETC to test for such modulations. Figures 6–8 show examples of JPETCs of three pairs of sites for different movement types. The JPETC matrix is displayed in colour code in the centre of each figure.

TABLE 2. Frequency of significant movement-related correlation changes

	Incidence of increases and decreases in correlation (%)					
	Within right hemisphere		Within left hemisphere		Between hemispheres	
	Incidence	(Diagonals)	Incidence	(Diagonals)	Incidence	(Diagonals)
Increases in correlation						
Monkey P						
All trial types	45.4	(1420)	38.9	(1331)	36.2	(3206)
Unimanual right movements	42.5	(518)	44.5	(483)	40.5	(1160)
Unimanual left movements	47.4	(519)	38.0	(487)	33.4	(1173)
Bimanual movements	46.5	(383)	32.7	(361)	34.0	(873)
Monkey G						
All trial types	52.5	(1563)	60.1	(1242)	58.7	(3553)
Unimanual right movements	56.7	(522)	63.0	(414)	58.1	(1184)
Unimanual left movements	58.2	(495)	56.0	(393)	58.2	(1126)
Bimanual movements	34.8	(678)	61.2	(435)	51.6	(1242)
Decreases in correlation						
Monkey P						
All trial types	77.1	(1420)	85.6	(1331)	80.1	(3206)
Unimanual right movements	79.3	(518)	86.8	(483)	81.0	(1160)
Unimanual left movements	78.2	(519)	89.3	(487)	85.0	(1173)
Bimanual movements	72.6	(383)	79.2	(361)	72.2	(873)
Monkey G						
All trial types	66.7	(1563)	68.6	(1242)	58.8	(3553)
Unimanual right movements	65.1	(522)	59.7	(414)	60.9	(1184)
Unimanual left movements	64.4	(495)	70.2	(393)	56.0	(1126)
Bimanual movements	70.1	(678)	75.6	(435)	59.2	(1242)

Frequency with which a significant change in correlation strength occurred in the main diagonal of the JPETC during the movement period as compared to the hold period. For each pair of sites, each movement type was considered separately. The number of diagonals from which the percentages were derived are shown in brackets.

We display the mEP of the two signals in each pair along the x and y axes. The main diagonal of the JPETC (the diagonal row of bins from the bottom left to the top right) represents the time course of zero-delay correlation and is displayed separately in the upper right corner of each figure. The time-averaged correlogram is derived by averaging the diagonals at a range of –200 to +200 ms delay.

It is worth emphasizing that the JPETC depicts the correlated activity after subtracting the mEP from each raw LFP single-trial signal (see Materials and Methods). The tests described in the methods section (Fig. 2) indicated that the correlations depicted by this procedure are not created by the patterns of mEPs. Rather, the correlation patterns reflect correlated intertrial variability of neuronal activity, which may arise from correlated noise at a given time, or from correlated time shifts of the neuronal signals.

In both monkeys, the majority of JPETCs contained significant changes along the main diagonal. In 57.4% (39.0%) of all diagonals from monkey G (monkey P), the JPETC revealed significant increases of correlation during the movement period as compared to the hold period. Significant decreases were observed in 62.6% (80.9%, monkey P) of the diagonals. Both increases and decreases could occur in the same JPETC. In many cases, additional features showed up on diagonals off the main diagonal. For instance, it was relatively common to see negative dips around elevated correlations at zero delay (Fig. 6A, C and D, and Fig. 7B). In some cases, oscillations with at least one additional positive side peak arose around movement onset (as in Fig. 7B). Profound changes of correlation strength could be found in JPETCs taken from pairs situated in the same hemisphere (Fig. 6), as well as those situated in different hemispheres (Figs 7 and 8).

Figure 6 shows four JPETCs from a pair of LFPs recorded in the left hemisphere during different types of movement. The figure shows that the two sites were correlated during all four movement types (red bins along the main diagonals, indicating positive correlations). However, comparing the plots of the JPETC diagonals, it becomes clear that differences existed in modulation strength. In the bimanual movements (Fig. 6C and D), a clear movement-related modulation of correlation is visible, consisting of a pronounced increase peaking at movement onset and followed by a small decrease. In unimanual movements, this correlation change was much weaker (Fig. 6A) or virtually absent (Fig. 6B). In the JPETC colour display of C and D, negative side dips and an additional oscillatory side peak appear around movement onset, corresponding to a frequency of just below 10 Hz. In contrast, strong synchronized oscillations in the gamma frequency are present during the hold period which are also visible in the averaged correlogram. These oscillations can be seen in the inset, depicting the area surrounded by the rectangle within Fig. 6A at an expanded scale. Note that the time scales of the averaged correlogram and the JPETC differ, so that the satellite peaks appear at a wider spacing in the correlograms and are thus more clearly discernible than in the JPETC. These gamma oscillations became much weaker during the reaction time (target onset was on average 270 ms before movement onset) and had totally disappeared when movements were initiated. The different movement types were presented in a random order, but at a fixed interval after origin onset. Thus, whilst the monkeys were able to predict the time when a new movement would be cued, they could not predict which specific movement would be instructed next. Therefore, the oscillations before target onset could be related to some nonspecific process of movement preparation or readiness, but not to the preparation of a specific movement. Note that, whilst the diagonals are different, the correlograms look quite similar in all conditions. Both LFP signals were significantly tuned ($r^2 > 0.6$) to movements to the right, with a difference in preferred direction of only 17°. The PD of electrode 4 was 351°, and the PD of electrode 6 was 8°.

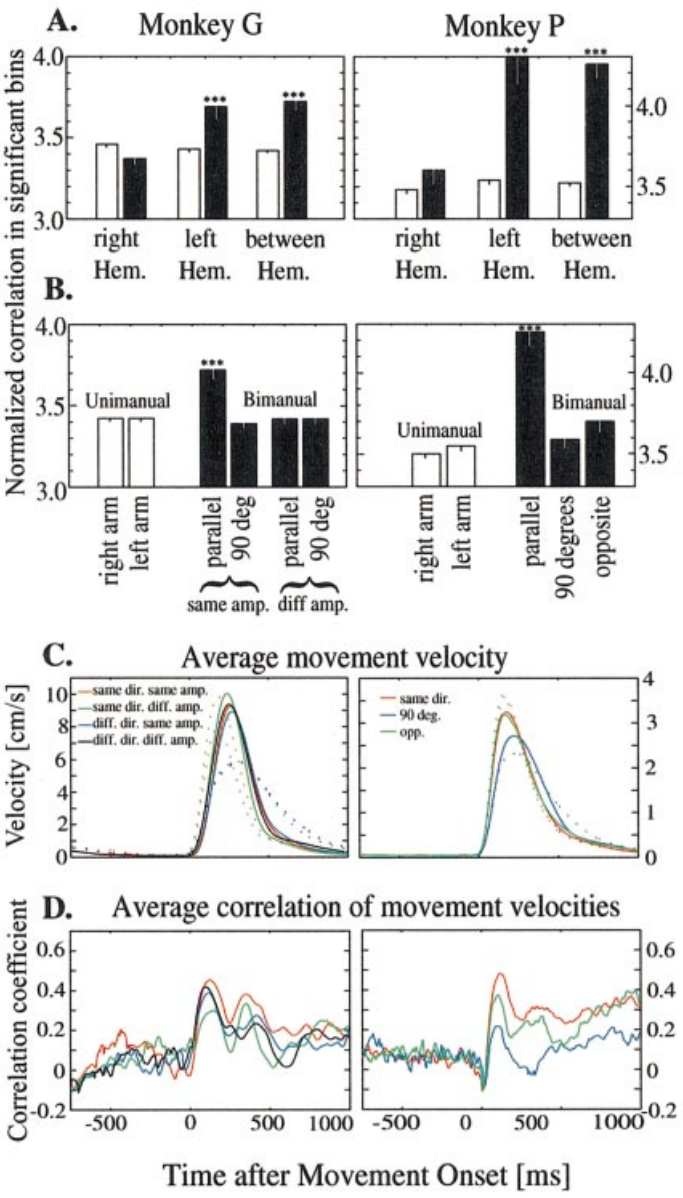

FIG. 9. (A and B) Average normalized size of significant increases of correlation revealed within the JPETC diagonals. The size of correlation changes has been normalized as described in the methods. (A) Comparison of correlation increases during all unimanual trial types (open bars) and all bimanual trial types (black bars). (B) Comparison of interhemispheric correlation increases in different types of movement. Lines at the end of each bar represent the SEM. Correlation increases of bimanual movements that differ significantly from the respective unimanual correlation changes are marked (Wilcoxon rank sum test, $***P < 0.001$). (C) Average velocity profiles (over all trials and all days) of the two arms (continuous line, left arm; dashed line, right arm) in the different bimanual movement types. Colours indicate the movement type executed. (D) Average JPETC diagonals (over all trials and days) of correlations between the velocities of the two arms in different bimanual movement types. Colours as in C.

Similar movement-related increases and decreases in correlation were also found interhemispherically (Fig. 7). In this example, there is no significant correlation change during unimanual movements (Fig. 7A), but a strong, brief correlation with an additional side peak arises around movement onset in bimanual movements (Fig. 7B). The time delay of this side peak is ≈ 100 ms, corresponding to a frequency of ≈ 10 Hz (i.e. in the alpha band). Similar to the example of Fig. 6, weak synchronized gamma oscillations were present during the hold period. Because of their relative weakness and the temporal resolution of the JPETC, however, they are barely visible in the colour display of the JPETC (lower left corner of the JPETC in Fig. 7B). Both the alpha and gamma components can be seen in the averaged correlogram. The diagonal runs first through a negative side dip, whereas it later straddles the main, positive peak. Therefore, the diagonal shows an initial decrease in correlation, followed by a later increase. The mEP on electrode 1 was not significantly tuned, but was most strongly activated during rightward movements of the contralateral arm. The mEP on electrode 4 was significantly tuned and had a preferred direction which was also to the right (351°).

Another example, this time demonstrating decorrelation, is shown in Fig. 8. This pair of sites was situated in different hemispheres of monkey P. The JPETC shows decorrelation both for unimanual (Fig. 8A) and bimanual movements (Fig. 8B). During the hold phase, negative side bands are present at relatively long delays (≈ 500–700 ms), which disappear during the movement and the decorrelation. Neither site was significantly cosine-tuned to the direction of movement.

In general, both the largest correlation values and the strongest correlation changes in our sample were seen along the main diagonal, i.e. at zero delay. Therefore, in the following analyses, we quantified the correlation changes over time along these diagonals. First, we analysed the frequency and size of correlation changes, and examined any differences among the different bimanual movement types. Then, we assessed the time course of correlation changes and the net correlation change observed over all recording sites.

Comparing the percentages of increased and decreased correlation

To assess how frequently one observes dynamic modulation of correlations, we counted the number of main JPETC diagonals that showed statistically significant changes of correlation strength (as compared to the hold period, for each pair and condition). The results are summarized in Table 2. The table illustrates a number of remarkable points. (i) Under all conditions, decreases of correlation strength were observed more frequently than increases. (ii) Interhemispheric pairs showed correlation increases and decreases in percentages that were similar to those shown in intrahemispheric pairs. This is in contrast to the averaged correlations, in which intrahemispheric correlations were stronger than interhemispheric ones. (iii) Intrahemispheric changes were observed during unimanual (both ipsilateral and contralateral) and bimanual arm movements. (iv) Interhemispheric pairs underwent dynamic correlation changes not only during bimanual, but also during unimanual movements.

The JPETC dynamics during different movement types

Table 2 does not show any systematic differences in correlation changes during different movement types. However, Table 2 only counts the incidence of correlation changes. In order to also compare the magnitude of correlation changes along different diagonals, we normalized the correlation scores as discussed in the Materials and Methods section. Normalized scores with absolute magnitude > 3 SD from the mean (indicating significant increase in a given bin, as compared to the hold period, with an error probability of 0.002) were considered significant. Figure 9A compares the average normalized correlation strength over all significant bins of all JPETC-diagonals during unimanual and bimanual movements. For interhemispheric and left hemisphere pairs of LFP signals (contralateral to the preferred right hand), bimanual movements elicited significantly stronger correlation increases than unimanual movements (Wilcoxon

TABLE 3. Differences between preferred directions

	Pairs with significant increases in correlation		Pairs with significant decreases in correlation		Pairs with no change in correlation	
	Same	Different	Same	Different	Same	Different
Monkey G	16.3°	43.3°	15.6°	43.3°	17.6°	54.9°
Monkey P	17.5°	35.3°	12.0°	34.0°	12.0°	32.6°

Medians of differences (in degrees) between the preferred directions of significantly cosine-tuned local field potentials (LFPs). Same, values of pairs within the same hemisphere; Different, values of pairs in different hemispheres. For each pair, all movement types have been considered separately.

signed rank test, $P < 0.001$). Between the hemispheres, there was also a systematic difference between different bimanual trial types: parallel movements of the same amplitude were accompanied by significantly higher correlation increases than those with different amplitudes or directions (Wilcoxon signed rank test, $P < 0.001$, Fig. 9B). The number of significantly increased bins per diagonal in interhemispheric pairs was also higher for bimanual parallel movements than for all other movement types (not shown). In contrast, no consistent differences between trial types were found in intrahemispheric pairs. Decreases in correlation did not show any differences in their strength when comparing different trial types or when comparing interhemispheric and intrahemispheric pairs.

To compare the correlations between the two hemispheres with correlations between the movements of the arms, we also applied the JPETC method to the velocities of both arms during bimanual movements (Fig. 9C). The average JPETC diagonals of this analysis is shown in Fig. 9D. Correlations between the arms increased strongly in the accelerating phase of the movements and decreased during the decelerating phase. The peak correlation between the arms occurred before movements had reached their velocity peak. Like the interhemispheric LFP correlations, in both monkeys, the correlations between the arms were significantly higher during bimanual symmetric movements of the same amplitude than in all other bimanual movement types (Wilcoxon signed rank test, $P < 0.001$).

Relationships between preferred directions and the incidence of correlation changes

For all electrodes, we determined whether the mEPs were cosine-tuned. We found that 27% of the LFPs in monkey G and 19% of the LFPs in monkey P were significantly cosine-tuned ($r^2 > 0.6$, see Materials and Methods). For those pairs in which both sites showed significant tuning, we determined the angles between the preferred directions and compared the distributions of these angles between pairs showing significant increases, decreases or no change in correlation (Table 3). We found no consistent differences between the distributions for these three groups. There was no relationship between the difference in directional tuning and the correlation changes.

Within the same hemisphere, the medians of the angles between preferred directions were small (with medians ranging between 12 and 18°), indicating that the strongly tuned sites within a distance of 350–700μm lateral distance usually had similar preferred directions. However, the fact that we also found pairs with considerably different PDs clearly suggests that the observed similarity cannot be explained solely on the basis of passive current spread. Pairs recorded from different hemispheres had consistently larger differences between preferred directions, with medians between 32 and 55°.

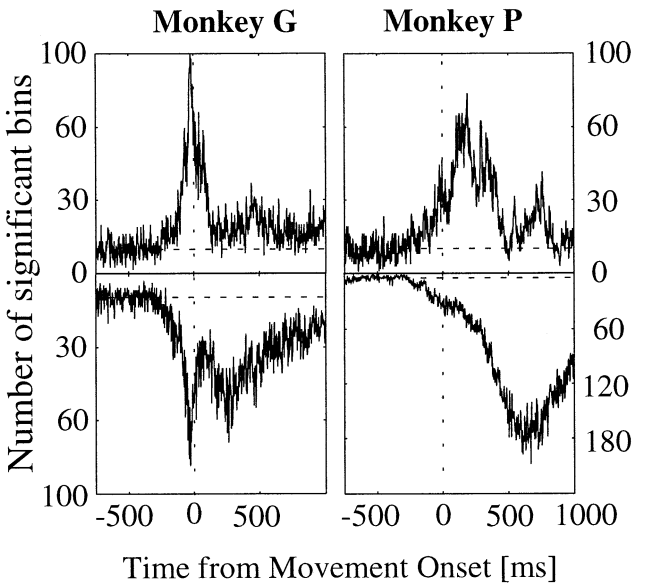

FIG. 10. Occurrence of significantly increased or decreased correlation (as compared to the hold period) in the JPETC diagonals. The number of significantly deviating correlations in each time bin is plotted on the *y*-axis. More than 2000 diagonals have been included in each plot. Because we did not find differences in the time courses of pairs within the same or different hemispheres, we show here the sum of both types of pairs. For better comparison of time courses, values for increases are plotted upwards and values for decreases are plotted downwards. The horizontal dashed line at time 0 indicates movement onset. The vertical dashed line indicates the average level of randomly occurring deviations in correlation during the hold period.

Time course of correlation changes

We analysed the time course of significant correlation changes separately for increases and decreases. For each 2.5-ms time bin, we determined whether significant correlation changes occurred and used these results to construct two indicator vectors for each pair of LFP signals and each trial type. The vectors contained zeros at those time bins where correlation had not changed significantly and ones at bins in which a significant increase (for the first vector) or decrease (for the second vector) had occurred. Figure 10 shows the sums of these vectors over all pairs, which represents the number of significant changes occurring for each time bin in the whole database. The sum of the increased-correlation vector is plotted upwards and the sum of the decreased-correlation vector is plotted downwards. Onset of both increases and decreases is similar at ≈200 ms before movement, corresponding to a time when the targets had already appeared on the screen. Increases in correlation were sharply peaked around movement onset. In contrast, decreases in correlation were more broadly distributed over the movement. Although in monkey G decorrelations also show a sharp initial peak shortly before movement onset, most of the decorrelations in both monkeys occurred after movements were initiated. In monkey P, both curves seem to be delayed in time as compared to those of monkey G. This may be related to the fact that the movement times of monkey P were much longer, so that the relevant time scale may have been expanded in this monkey. Repeating this procedure separately for inter- and intrahemispheric pairs and for different movement types did not reveal any systematic differences.

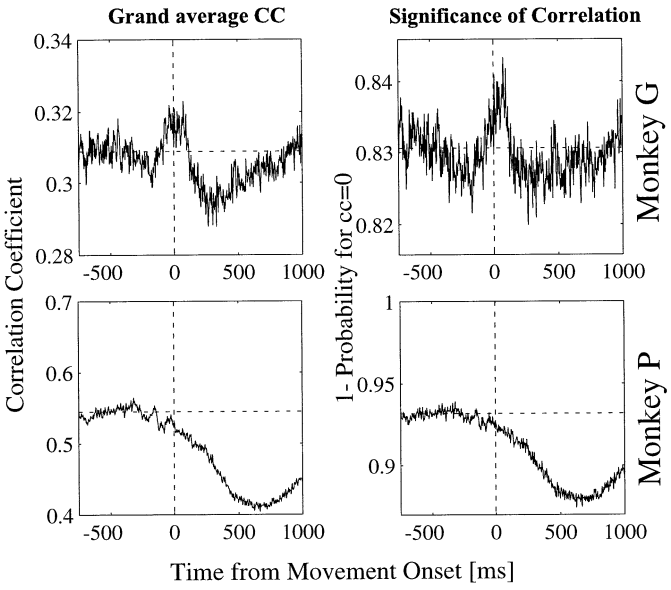

FIG. 11. Grand average of all JPETC diagonals (within and between hemispheres, including all movement types). (A) Average of all diagonals expressed in the correlation coefficient. (B) Average of all diagonals expressed as significance of the correlation coefficient. The significance is given as (1–*P*), where *P* is the probability of the correlation coefficient being statistically indistinguishable from 0. Significance was determined for the absolute values of correlation coefficients. The horizontal dashed line shows the average level in the hold period, the vertical dashed line indicates the time of movement onset.

The net correlation change during movements

Table 2 shows that decreased correlations occurred more often than increases. To test whether the decorrelations outweighed the increases, we calculated the grand average of correlations between all recording site pairs as shown in Fig. 11, either expressed as the correlation coefficient (Fig. 11A) or as the significance of the correlation coefficient (Fig. 11B). Indeed, the figure shows that, on average, the correlation decreased during the movement. In monkey G, this decrease was smaller and, in addition, there was a short epoch around movement onset during which the correlation was on the average increased. We found no differences between the grand average correlation changes in different movement types and in intra- vs. interhemispheric pairs.

Discussion

This study tested whether interactions between neuronal populations, especially between the hemispheres, might play a role in coordinated bimanual arm movements. In order to investigate this question, we used correlational approaches to detect functional interactions and examine how they change over time and how they are related to behaviour.

Time-averaged LFP correlations between the hemispheres were significantly smaller than those within the same hemisphere, suggesting that interhemispheric interactions are less intense than intrahemispheric ones. This is in agreement with EEG studies, which have reported only weak interhemispheric correlations (Schoppenhorst *et al*., 1980; Andrew & Pfurtscheller, 1997, 1999). Although weak, many correlations recorded between the hemispheres were still significant, confirming earlier reports that interhemispheric correlations of single cells and LFPs do exist and are not negligible (Munk *et al*., 1995; Murthy & Fetz, 1996).

Time-averaged correlations did not differ between the hold period and the different movement types (Fig. 5). In order to address the possibility that this was a result of time averaging, we sought to reveal time-dependent modulations of interactions. To this end, we modified the JPSTH technique developed by Aertsen *et al*. (1989). The JPSTH detects dynamic modulation of interactions in relation to specific events (Eggermont, 1994; Sillito *et al*., 1994; Vaadia *et al*., 1995; Prut *et al*., 1998). We adapted the procedure for use with analogue data and called it the JPETC. It offers a temporal resolution in the ms range and is applied here for the first time on LFP data. Previous analyses of time-resolved correlation or coherence of analogue signals focused on sliding-window techniques (e.g. Bressler *et al*., 1993; Roelfsema *et al*., 1997; Destexhe *et al*., 1999), which suffer from a limited temporal resolution. In contrast to event-related coherence measures, the JPETC can also detect nonperiodic correlations.

In the methods section, we demonstrated that the JPETC is not contaminated by the sizes or shapes of the mEPs, or by overall changes in variability. It rather reveals correlations between the trial-by-trial fluctuations of the two LFP signals around the mEPs, but may also reflect covariations in signal timing. Both phenomena are interesting, because they reveal functional links between distant sites within the motor cortex or even between hemispheres. The context-dependence of these functional links demonstrates the dynamics of this system and its relationship to behaviour. Covariations in signal timing can be seen as evidence for a common timing linking distant neuronal sites.

The JPETC revealed movement-related correlations in a majority of pairs, suggesting that most neural interactions are flexible and are regulated in relation to movements. Although the average levels of correlation differed, intra- and interhemispheric pairs showed similar fractions and strengths of movement-related correlation changes. This indicates that interactions between the hemispheres are as strongly modulated as those within the same hemisphere.

Changes in correlation could consist of increases or decreases, and a given pair could show different patterns of correlation changes for different kinds of movements. This raises the possibility that the strength of correlation may carry some information about the type of movement to be executed. Variable correlations, changing with behavioural conditions or events, have also been reported in single neurons from precentral areas (Vaadia *et al*., 1995) and motor cortex (Murthy & Fetz, 1996; Riehle *et al*., 1997; Hatsopoulos *et al*., 1998; Grammont & Riehle, 1999; Laubach *et al*., 2000). One group specifically claimed that the information contained in correlations improve coding of movement direction (Maynard *et al*., 1999). Our findings show that, although the LFP signal is certainly less specific than single cell-activity, LFP correlations (in addition to mEP amplitudes) may convey behaviourally relevant information.

Concerning the question of whether interhemispheric interactions aid bimanual coordination, the most striking result of this study was that interhemispheric correlations (but not intrahemispheric ones) were consistently related to the degree of bimanual coupling. Symmetric bimanual movements were accompanied by significantly stronger correlation increases than asymmetric bimanual or unimanual movements. At the same time, the correlations between the movements of the two arms themselves were also highest for bimanual symmetric movements of the same amplitude. This suggests that interhemispheric correlations contribute to interlimb coupling and aid in production of bimanually symmetric movements. By the same token, interhemispheric coupling may underlie the

difficulties we have in producing asymmetric movements. The significantly weaker correlation increases that we found during asymmetric movements may be the result of an active process that reduces coupling, and the residual correlations may be a neural correlate of our inability to completely decouple our arms. This idea is also in line with the finding that split-brain patients (in which the callosal connections have been destroyed) are better than normal individuals in strongly asymmetric bimanual tasks (Eliassen *et al*., 1999). Thus, our findings are consistent with the view that interhemispheric correlations are the functional basis of crosstalk between the motor plans for the two hands, and regulation of the strength of this crosstalk may determine the level of behavioural coupling between the arms.

The time course of correlation changes lends further support to this notion. Because modulations of correlation began before movement onset, it is feasible that they are related to movement programming or preparation rather than execution. This would be consistent with the observation that interlimb crosstalk occurs even when a movement is not actually executed, such as when it is only imagined (Heuer *et al*., 1998b), or when a limb has been amputated (Franz & Ramachandran, 1998). Like the increased correlations described in this study, crosstalk between two simultaneously planned movements occurs during a transient phase associated with the process of movement preparation (Heuer *et al*., 1998a).

Finally, it is noteworthy that pairs within the same hemisphere also showed movement-related correlation increases during bimanual movements. This raises the possibility that intrahemispheric interactions may also participate in bimanual control. Although this may seem odd, there are other recent results that support this hypothesis. There is growing evidence of significant ipsilateral activation of the motor cortex (Tanji *et al*., 1988; Donchin *et al*., 1998; Kermadi *et al*., 1998; for review, see Chen *et al*., 1997). Furthermore, firing rates of MI cells are different during bimanual and unimanual reaching, supporting the suggestion that neurons in each hemisphere are related to the movement of both arms (Donchin *et al*., 1998). Finding inter- and intrahemispheric interactions during bimanual movements is further evidence of the fact that both hemispheres seem to be involved in movements of both arms.

Besides the increases in LFP correlations that have been discussed above, we also observed decreases in correlation. However, whilst increases in LFP correlations occurred mainly during movement planning and initiation (around movement onset), decreases occurred mainly during movement execution. As a result of this timing difference, the net correlation change after movement initiation was a decrease. Decreased correlations were found relatively uniformly in all movement types, and are an oft-reported phenomenon in population activity (Sanes & Donoghue, 1993; MacKay & Mendonca, 1995; Baker *et al*., 1997; Donoghue *et al*., 1998; Pfurtscheller & Lopes da Silva, 1999). The different time course of increased and decreased correlations could explain the behavioural finding that bimanual movements are most closely coupled at their initiation and are progressive desychronized during movement execution (Boessenkool *et al*., 1999; Fowler *et al*., 1991). The overall picture would then be that increases in LFP correlations are involved in crosstalk during movement planning and initiation, and decreased correlation serves to decouple movements during their execution.

Previously, we had reported that firing rates and mEP amplitudes in primary motor cortex are bimanually related and thus may contribute to the coding of coordinated bimanual movements (Donchin *et al*., 1998; Donchin *et al*., 2001). Now, we show that dynamic interactions between neuronal populations are also involved in this function. We conclude that flexible interhemispheric correlations may be the neuronal substrate controlling the level of behavioural coupling between the arms.

Acknowledgements

The research was supported in part by the Israel Science Foundation, founded by the Israel Academy of Sciences and Humanities, the United States–Israel Binational Science Foundation, the German–Israeli Foundation for Scientific Research and Development (GIF) and the DFG (CA 245/1-1). We thank the MINERVA foundation that supported S.C.d.O. as a postdoctoral fellow and the Clore Foundation for a fellowship to O.D. During part of the data analysis, S.C.d.O. was a fellow of the Hanse Institute for Advanced Studies, Delmenhorst, and enjoyed the hospitality of K. Pawelzik at the Institute of Theoretical Physics, University Bremen. We also thank G. Goelman for obtaining the MRI pictures, A. Arieli for developing an algorithm for movement onset detection, and K. Pawelzik for helpful discussions and comments. Histological evaluation was performed in collaboration with S. Haber (University of Rochester, USA). Additionally, the suggestions made by two anonymous referees helped to substantially improve the manuscript.

Abbreviations

IAI, inter-arm interval; JPETC, joint peri-event time correlogram; LFP, local field potential; mEP, mean motor evoked potential; PD, preferred direction.

References

Aertsen, A.M., Gerstein, G.L., Habib, M.K. & Palm, G. (1989) Dynamics of neuronal firing correlation: modulation of 'effective connectivity. *J. Neurophysiol.*, **61**, 900–917.

Andres, F.G., Mima, T., Schulman, A.E., Dichgans, J., Hallett, M. & Gerloff, C. (1999) Functional coupling of human cortical sensorimotor areas during bimanual skill acquisition. *Brain*, **122**, 855–870.

Andrew, C. & Pfurtscheller, G. (1997) On the existence of different alpha band rhythms in the hand area of man. *Neurosci. Lett.*, **222**, 103–106.

Andrew, C. & Pfurtscheller, G. (1999) Lack of bimanual coherence of post-movement central beta oscillations in the human electroencephalogram. *Neurosci. Lett.*, **273**, 89–92.

Arieli, A., Shoham, D., Hildesheim, R. & Grinvald, A. (1995) Coherent spatiotemporal patterns of ongoing activity revealed by real-time optical imaging coupled with single-unit recording in cat visual cortex. *J. Neurophysiol.*, **73**, 2072–2093.

Arieli, A., Sterkin, A., Grinvald, A. & Aertsen, A. (1996) Dynamics of ongoing activity: explanation of the large variability in evoked cortical responses. *Science*, **273**, 1868–1871.

Baker, S.N. & Gerstein, G.L. (2001) Determination of response latency and its application to normalization of cross-correlation measures. *Neural Computation*, **13**, 1351–1377.

Baker, S.N., Olivier, E. & Lemon, R.N. (1997) Coherent oscillations in monkey motor cortex and hand muscle EMG show task-dependent modulation. *J. Physiol. (Lond.)*, **501**, 225–241.

Ben-Shaul, Y., Bergman, H., Ritov, Y. & Abeles, M. (2001) Trial to trial variability in either stimulus or action causes apparent correlation and synchrony in neuronal activity. *J. Neurosci. Meth.*, **111**, 99–110.

Boessenkool, J.J., Nijhof, E.-J. & Erkelens, C.J. (1999) Variability and correlations in bi-manual pointing movements. *Hum. Movment Sci.*, **18**, 525–552.

Bressler, S., Coppola, R. & Nakamura, R. (1993) Episodic multiregional cortical coherence at multiple frequencies during visual task performance. *Nature*, **366**, 153–156.

Brody, C.D. (1999) Correlations without synchrony. *Neural Computation*, **11**, 1537–1551.

Cardoso de Oliveira, S., Gribova, A., Donchin, O., Bergman, H. & Vaadia, E. (2000) Interhemispheric correlations between populations of precentral motor cortex during bimanual arm movements. *Soc. Neurosci. Abstr.*, **26**, 1482.

Chen, R., Cohen, L. & Hallett, M. (1997) Role of the ipsilateral motor cortex in voluntary movement. *Can. J. Neurol. Sci.*, **24**, 284–291.

Destexhe, A., Contreras, D. & Steriade, M. (1999) Spatiotemporal analysis of

local field potentials and unit discharges in cat cerebral cortex during natural wake and sleep states. *J. Neurosci.*, **19**, 4595–4608.
Donchin, O., Cardoso de Oliveira, S. & Vaadia, E. (1999) Who tells one hand what the other is doing: the neurophysiology of bimanual movements. *Neuron*, **23**, 15–18.
Donchin, O., Gribova, A., Steinberg, O., Bergman, H., Cardoso de Oliveira, S. & Vaadia, E. (2001) Local field potentials related to bimanual movements in the primary and supplementary motor cortices. *Exp. Brain Res.*, **140**, 46–55.
Donchin, O., Gribova, A., Steinberg, O., Bergman, H. & Vaadia, E. (1998) Primary motor cortex is involved in bimanual coordination. *Nature*, **395**, 274–278.
Donoghue, J.P., Sanes, J.N., Hatsopoulos, N.G. & Gaal, G. (1998) Neural discharge and local field potential oscillations in primate motor cortex during voluntary movements. *J. Neurophysiol.*, **79**, 159–173.
Eggermont, J.J. (1994) Neural interaction in cat primary auditory cortex II. Effects of sound stimulation. *J. Neurophysiol.*, **71**, 246–270.
Eliassen, J.C., Banes, K. & Gazzaniga, M.S. (1999) Direction information coordinated via the posterior third of the corpus callosum during bimanual movements. *Exp. Brain Res.*, **128**, 573–577.
Eliassen, J.C., Baynes, K. & Gazzaniga, M.S. (2000) Anterior and posterior callosal contributions to simultaneous bimanual movements of the hands and fingers. *Brain*, **123**, 2501–2511.
Fowler, B., Duck, T., Mosher, M. & Mathieson, B. (1991) The coordination of bimanual aiming movements: evidence for progressive desynchronization. *Quart. J. Exp. Psychol.*, **43**, 205–221.
Franz, E. (1997) Spatial coupling in the coordination of complex actions. *Quart. J. Exp. Psychol.*, **50A**, 684–704.
Franz, E.A., Eliassen, J.C., Ivry, R.B. & Gazzaniga, M.S. (1996) Dissociation of spatial and temporal coupling in the bimanual movements of callosotomy patients. *Psychol. Sci.*, **7**, 306–310.
Franz, E.A. & Ramachandran, V.S. (1998) Bimanual coupling in amputees with phantom limbs. *Nature Neurosci.*, **1**, 443–444.
Franz, E.A., Waldie, K.E. & Smith, M.J. (2000) The effect of callosotomy on novel versus familiar bimanual actions: a neural dissociation between controlled and automatic processes?. *Psychol. Sci.*, **11**, 82–85.
Grammont, F. & Riehle, A. (1999) Precise spike synchronization in monkey motor cortex involved in preparation for movement. *Exp. Brain Res.*, **128**, 118–122.
Hatsopoulos, N.G., Ojakangas, C.L., Paninski, L. & Donoghue, J.P. (1998) Information about movement direction obtained from synchronous activity of motor cortical neurons. *Proc. Natl Acad. Sci. USA*, **95**, 15706–15711.
Heuer, H., Spijkers, W., Kleinsorge, T., van der Loo, H. & Steglich, C. (1998a) The time-course of cross-talk during the simultaneous specification of bimanual movement amplitudes. *Exp. Brain Res.*, **118**, 381–392.
Heuer, H., Spijkers, W., van Kleinsorge, T. & derLoo, H. (1998b) Period duration of physical and imaginary movement sequences affects contralateral amplitude modulation. *Q. J. Exp. Psychol.*, **51**, 755–779.
Kelso, J.A.S. (1984) Phase transitions and critical behavior in human bimanual coordination. *Am. J. Phys.*, **246**, R1000–R1004.
Kelso, J.A., Southard, D.L. & Goodman, D. (1979) On the coordination of two-handed movements. *J. Exp. Psychol.*, **5**, 229–238.
Kermadi, I., Liu, Y., Tempini, A., Calciati, E. & Rouiller, E.M. (1998) Neuronal activity in the primate supplementary motor area and the primary motor cortex in relation to spatio-temporal bimanual coordination. *Somatosens. Mot. Res.*, **15**, 287–308.
Laubach, M., Wessberg, J. & Nicolelis, M.A. (2000) Cortical ensemble activity increasingly predicts behaviour outcomes during learning of a motor task. *Nature*, **405**, 567–571.
MacKay, W.A. & Mendonca, A.J. (1995) Field potential oscillatory bursts in parietal cortex before and during reach. *Brain Res.*, **704**, 167–174.
Maynard, E.M., Hatsopoulos, N.G., Ojakangas, C.L., Acuna, B.D., Sanes, J.N., Normann, R.A. & Donoghue, J.P. (1999) Neuronal interactions improve cortical population coding of movement direction. *J. Neurosci.*, **19**, 8083–8093.
Mitzdorf, U. (1994) Properties of cortical generators of event-related potentials. *Pharmacopsychiatry*, **27**, 49–51.
Munk, M.H.J., Nowak, L.G., Nelson, J.I. & Bullier, J. (1995) Structural basis of cortical synchronization. II. Effects of cortical lesions. *J. Neurophysiol.*, **74**, 2401–2414.
Murthy, V. & Fetz, E.E. (1996) Synchronization of neurons during local field potential oscillations in sensorimotor cortex of awake monkeys. *J. Neurophysiol.*, **76**, 3968–3982.
Pfurtscheller, G. & Lopes da Silva, F.H. (1999) Event-related EEG/MEG synchronization and desynchronization: basic principles. *Clin. Neurophysiol.*, **110**, 1842–1857.
Preilowski, B.F.B. (1972) Possible contribution of the anterior forebrain commissures to bimanual motor coordination. *Neuropsychologia*, **10**, 267–277.
Preilowski, B.F.B. (1975) Bimanual motor interaction: perceptual–motor performance of partial and complete 'split-brain' patients. In Zulch, K.J., Creutzfeld, O. & Galbraith, G.C. (eds), *Cerebral Localization*. Springer, New York, pp. 115–132.
Prut, Y., Vaadia, E., Bergman, H., Haalman, I., Slovin, H. & Abeles, M. (1998) Spatiotemporal structure of cortical activity: properties and behavioral relevance. *J. Neurophysiol.*, **79**, 2857–2874.
Riehle, A., Gruen, S., Diesmann, M. & Aertsen, A. (1997) Spike synchronization and rate modulation differentially involved in motor cortical function. *Science*, **278**, 1950–1953.
Roelfsema, P.R., Engel, A.K., Koenig, P. & Singer, W. (1997) Visuomotor integration is associated with zero time-lag synchronization among cortical areas. *Nature*, **385**, 157–161.
Sanes, J. & Donoghue, J.P. (1993) Oscillations in local field potentials of the primate motor cortex during voluntary movement. *Proc. Natl Acad. Sci. USA*, **90**, 4470–4474.
Schoppenhorst, M., Brauer, F., Freund, G. & Kubicki, S. (1980) The significance of coherence estimates in determining central alpha and mu activities. *Electroencephalogr. Clin. Neurophysiol.*, **48**, 25–33.
Sillito, A.M., Jones, H.E., Gerstein, G.L. & West, D.C. (1994) Feature-linked synchronization of thalamic relay cell firing induced by feedback from the visual cortex. *Nature*, **369**, 479–482.
Tanji, J., Okano, K. & Sato, K.C. (1987) Relation of neurons in the nonprimary motor cortex to bimanual hand movement. *Nature*, **327**, 618–620.
Tanji, J., Okano, K. & Sato, K.C. (1988) Neuronal activity in cortical motor areas related to ipsilateral, contralateral, and bimanual digit movements of the monkey. *J. Neurophysiol.*, **60**, 325–343.
Tsodyks, M., Kenet, T., Grinvald, A. & Arieli, A. (1999) Linking spontaneous activity of single cortical neurons and the underlying functional architecture. *Science*, **286**, 1943–1946.
Tuller, B. & Kelso, J.A.S. (1989) Environmentally-specified patterns of movement coordination in normal and split-brain subjects. *Exp. Brain Res.*, **75**, 306–316.
Vaadia, E., Haalman, I., Abeles, M., Bergman, H., Prut, Y., Slovin, H. & Aertsen, A. (1995) Dynamics of neuronal interactions in monkey cortex in relation to behavioral events. *Nature*, **373**, 515–518.